https://doi.org/10.1590/jatm.v16.1344 ORIGINAL PAPER

Nonlinear Guidance Laws for Anti-tank Guided Missile to Intercept Maneuvering Tank Targets Using Optimal Error Dynamics and Relative Virtual Model

Hai Tran Van[1,*], Dien Nguyen Ngoc[1], Dung Pham Trung[1], Tung Thanh Nguyen[1]

1.Le Quy Don Technical University – Institute of Missile and Control Engineering – Hanoi – Viet Nam.

***Correspondence author:** tranvanhai@lqdtu.edu.vn

ABSTRACT

This paper introduces a new method for synthesizing guidance laws for anti-tank guided missiles (ATGM) to intercept maneuvering tank targets. It utilizes a nonlinear relative model in the two-dimensional horizontal plane and optimal error dynamics (OED) theory. The nonlinear relative model simplifies the problem of targeting a moving target into attacking a stationary target, making the guidance law synthesis task easier. The selection of OED allows for the design of a guidance command that ensures the zero effort miss (ZEM) error decreases to zero within a finite time, ensuring successful target interception. The paper also introduces an exponential decay weighting function of remaining time-to-go to optimize the distribution of command accelerations throughout the guidance process, thereby reducing initial command requirements and converging acceleration commands towards zero at the end time. The synthesized guidance laws are derived based on the nonlinear relative model and OED without making any small-angle linearization assumptions, allowing them to address various nonlinear scenarios. Numerical simulations illustrate the proposed guidance law's performance.

Keywords: Anti-tank guided missile; Guidance law; Optimal error dynamics; Nonlinear relative model.

INTRODUCTION

The design of missile guidance laws is a finite-time tracking issue aimed at achieving specific performance criteria. The focus is often on ensuring successful target interception, wherein the tracking error can be defined by two primary metrics: the zero effort miss (ZEM) (Dwivedi *et al.* 2016; He and Lee 2017) or the line-of-sight (LOS) rate (Zhou *et al.* 2009). By effectively nullifying the ZEM or LOS rate, a missile can achieve perfect interception capabilities. Among the strategies for missile guidance, proportional navigation guidance (PNG) stands out as a pioneering and widely applied technique. For decades, its variations have been vital in guiding missiles (Becker 1990; Zarchan 2012). The core principle of PNG involves generating lateral acceleration to nullify any changes in the LOS rate, ensuring that the missile maintains a collision course to intercept its target. However, PNG often requires large acceleration commands to intercept maneuvering targets, especially in the final phase.

To address this issue, augmented PNG (APNG) was developed using information about the target's acceleration to improve interception performance against moving targets. To study the synthesis of PNG and APNG laws using linear optimal control

Received: Jan 16 2024 | **Accepted:** Jul 24 2024
Peer Review History: Single Blind Peer Review.
Section editor: Luiz Martins-Filho

theory, we must simplify these kinematic equations appropriately. This can be achieved using small-angle assumptions (such as a slight heading error [HE] angle) to linearize these kinematic equations (Zarchan 2012). These limitations reduce their effectiveness in practical applications, especially when large initial heading angle deviations result in limited coverage of nonlinear engagement scenarios. The development of new guidance laws must consider nonlinear factors to enhance effectiveness and accuracy in all engagement situations, ensuring optimal interception capability in practice.

In developing advanced guidance laws, numerous optimal guidance laws have been introduced with the core goal of successful target interception and meeting additional requirements such as specific impact time or impact angle (Bin *et al.* 2023; He *et al.* 2017; Lee and Kim 2021; Lee *et al.* 2013; Ratnoo and Ghose 2010; Tran Van *et al.* 2023). For impact angle requirements, the intercept angle error is treated as the tracking error in the guidance law design (Van *et al.* 2023). However, most of these studies focus on fixed or nonmaneuvering targets, leaving a gap in research on maneuvering targets in nonlinear environments. The exploration and development of effective guidance laws for maneuvering targets in nonlinear contexts remain an area requiring deeper investigation.

After identifying the tracking error for a particular missile guidance problem, nonlinear control theories can be applied to reduce this error to zero within a specified timeframe. This process begins by selecting the desired error dynamics and constructing the control inputs to ensure that the system's trajectory converges to these selected error dynamics. This is a standard procedure for establishing new missile guidance laws using nonlinear control methods. However, most previous studies have focused on converging the tracking error to zero without considering the optimal error dynamics (OED) of a meaningful performance index (He *et al.* 2020). The PNG guidance law proves to be effective when utilized with a navigation constant ranging from 3 to 5, thereby improving overall robustness. However, maintaining this constant throughout the guidance process can require large normal accelerations when there is a significant initial HE. This phenomenon can overload the autopilot system and disturb the missile seeker. Therefore, a guidance law should reduce sensitivity to initial errors in fully homing guidance, facilitate seamless transitions, and prevent abrupt changes in combined guidance systems.

This paper introduces a method to solve the homing guidance problem for the anti-tank guided missile (ATGM) targeting a maneuvering tank using nonlinear kinematics on a horizontal plane. Unlike previous research, we employ a relative coordinate system attached to the target, with the origin at the target itself. By applying vector transformations, such as vector translation, we align the target's velocity, lateral acceleration, and axial acceleration vectors with the missile's velocity and acceleration vectors at a common origin attached to the missile. Subsequently, by utilizing vector addition and subtraction rules, we transform the initial problem into one where a missile with varying velocity attacks a stationary target. This method avoids relying on linear approximations, making the guidance law applicable to various nonlinear combat scenarios and facilitating practical implementation. Additionally, the paper introduces a time-to-go weighted power function to adjust the distribution of command acceleration throughout the guidance process. By adjusting the N_p guidance gain, this function reduces sensitivity to large initial HE angles.

Problem formulation and preliminaries

Engagement kinematics

The homing guidance method demonstrates the missile control law, represented as an algorithm constructed based on the dynamic geometrical correlations between the missile and the target. The homing guidance law is a mathematical equation (or system of equations) that expresses the dynamic geometrical relationship and motion parameters between two objects, allowing for the generation of control parameters to ensure the missile accurately approaches the target. Therefore, we first need to examine the dynamic geometrical correlation between the missile and the target to develop a guidance law for a homing missile.

Figure 1 illustrates the engagement geometry dynamics between the missile and the target in a two-dimensional horizontal plane model OX_IZ_I.

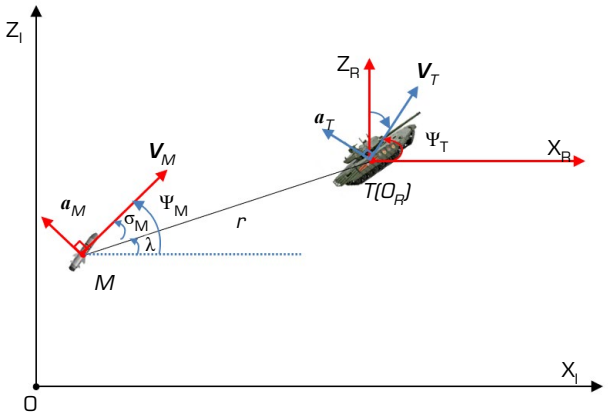

Source: Elaborated by the authors.

Figure 1. The kinematics of the missile and target in the horizontal plane.

In a 2D plane, the missile M and target T are modeled as point masses. Their velocity vectors are V_M for the missile and V_T for the target, with respective positions (x_M, z_M) and (x_T, z_T) in the inertial coordinate system. The angles of interest are the LOS angle, the missile's heading angle λ, Ψ_M, and the target's heading angle Ψ_T. Also, r is the range between the target and the missile. The lateral accelerations perpendicular to their trajectories are a_M for the missile and a_T for the target. The magnitudes of these vectors are V_M, V_T, a_M, and a_T, assuming that $V_M > V_T$. To simplify the problem, we assume that the axial acceleration component vector A_T aligns with the direction of the target's velocity vector. The lateral acceleration a_T characterizes the change in the direction of the velocity, while the axial acceleration A_T, which aligns with the velocity vector, signifies the increase in the tank's speed. The paper concentrates on formulating the guidance law, assuming that the target's maneuvering information is already known. Consequently, the estimation process of the target's information is beyond the scope of this paper.

The kinematic equations in the Cartesian inertial frame of the missile are:

$$\dot{x}_M = V_M cos\psi_M \tag{1}$$

$$\dot{z}_M = V_M \sin\psi_M \tag{2}$$

$$\sigma_M = \theta_M - \lambda \tag{3}$$

The position components, velocity, and velocity orientation of the tank vehicle, modeled as a point mass, are described by Eqs. 4–6:

$$\dot{x}_T = V_T cos\psi_T \tag{4}$$

$$\dot{z}_T = V_T \sin\psi_T \tag{5}$$

$$\dot{V}_T = A_T \tag{6}$$

The set of equations that describe the geometric dynamic relationship between the missile and the target is as follows:

$$\dot{r} = V_T cos(\psi_T - \lambda) - V_M cos(\psi_M - \lambda) \tag{7}$$

$$\dot{\lambda} r = V_T \sin(\psi_T - \lambda) - V_M \sin(\psi_M - \lambda) \tag{8}$$

$$\dot{\psi}_M = \frac{a_M}{V_M} \tag{9}$$

$$\dot{\psi}_T = \frac{a_T}{V_T} \tag{10}$$

The initial conditions are provided as follows: $r(0) = r_0$, $\lambda(0) = \lambda_0$, $\Psi_M(0) = \Psi_{M0}$, and $\Psi_T(0) = \Psi_{T0}$, respectively. To streamline the tracking model for intercepting a maneuvering target, we introduce a novel inertial coordinate system with its origin fixed to the target, as illustrated in Fig. 1. This makes the initial maneuvering target equivalent to a stationary virtual target (Jeon *et al.* 2015). Figure 2 depicts the geometric relationship between vectors V_M, V_T, a_M, a_T, and A_T in the inertial coordinate system and V_R, a_R the relative virtual coordinate system. Using vector translation, we align the target's velocity, lateral acceleration, and axial acceleration vectors with the missile's velocity and acceleration vectors at a common origin.

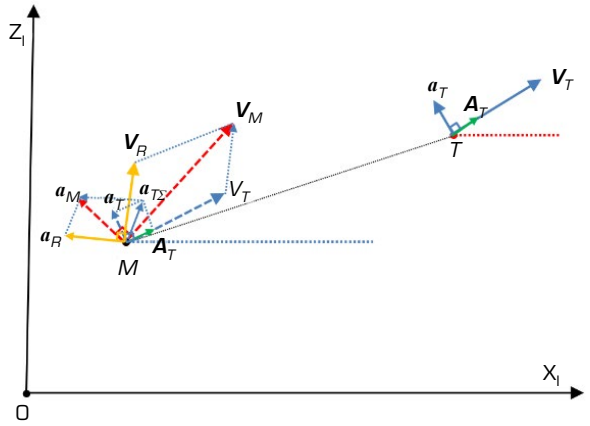

Source: Elaborated by the authors.

Figure 2. Geometric relationship between acceleration and velocity vectors of missile and target.

Then, by applying vector addition and subtraction rules, we obtain the following calculations: $V_R \triangleq V_M - V_T$ represents the relative velocity and $a_R \triangleq a_M - a_{T\Sigma}$ signifies the relative lateral acceleration command perpendicular to V_R, in which $a_{T\Sigma} \triangleq a_T + A_T$ is the sum of the target's lateral acceleration and axial acceleration vectors. The magnitudes of the vectors V_R and a_R are denoted as V_R and a_R, respectively. The geometric dynamic relationship between the missile and the target in the relative virtual coordinate system is precisely illustrated with rotation angles in Fig. 3.

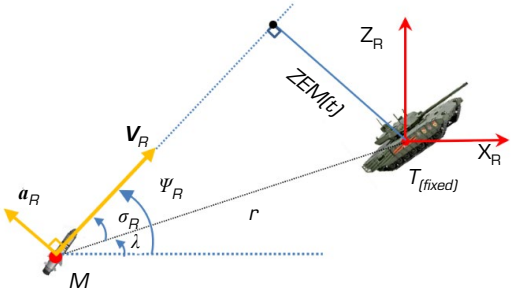

Source: Elaborated by the authors.

Figure 3. Geometric relationship in the relative virtual coordinate systems.

In the nonlinear virtual relative coordinate system, Ψ_R denotes the relative heading angle, and $\sigma_R = \Psi_R - \lambda$ defines a virtual look angle, the angle formed between the relative velocity V_R and the LOS.

Based on the dynamic geometric relationships illustrated in Figs. 1–3, we can determine the values for the relative velocity and heading angle in the relative virtual coordinate system as follows (Bin *et al.* 2023):

$$V_R = \sqrt{V_M^2 + V_T^2 - 2V_M V_T \cos(\psi_M - \psi_T)} \tag{11}$$

$$\psi_R = \tan^{-1} \frac{\sin\psi_M - \eta \sin\psi_T}{\cos\psi_M - \eta \cos\psi_T} \tag{12}$$

Let the velocity ratio be defined as $\eta = V_T / V_M$, where $\eta < 1$. Note that the relationship between the flight angles Ψ_M and Ψ_T in the original coordinate system and the relative heading angle Ψ_R in the new virtual coordinate system is provided by (Jeon *et al.* 2015):

$$\psi_M = \psi_R + \cos^{-1}\left(\frac{1 - \eta^2 + (V_R^2 / V_M^2)}{2V_R / V_M}\right) \tag{13}$$

$$\psi_T = \psi_M - \cos^{-1}\left(\frac{1 - \eta^2 + (V_R^2 / V_M^2)}{2V_R / V_M}\right) \tag{14}$$

Based on the geometric relationship of relative motions, the missile's normal acceleration in the relative coordinate system is calculated based on the missile's lateral acceleration, the target's lateral acceleration, and the target's axial acceleration, as defined below:

$$a_R = a_M \cos(\psi_R - \psi_M) - a_T \cos(\psi_R - \psi_T) + A_T \sin(\psi_R - \psi_T) \tag{15}$$

The kinematic and geometrical dynamic equations in the relative virtual reference frame shown in Fig. 3 are derived as follows:

$$\dot{r} = -V_R cos\sigma_R \tag{16}$$

$$\dot{\lambda} = \frac{-V_R \sin\sigma_R}{r} \tag{17}$$

$$\dot{\psi}_R = \frac{a_R}{V_R} \tag{18}$$

$$\dot{\sigma}_R = \dot{\psi}_R - \dot{\lambda} \tag{19}$$

To successfully intercept the target, the range r must decrease to *0* within a finite time t_f. Furthermore, from Eq. 17, it is observed that the virtual lead angle $\sigma_R(t)$ in the relative coordinate system must also be *0* to avoid situations where the rate of change of the LOS angle becomes infinite as r approaches *0*. From Eq. 16, for $r(t)$ to strictly decrease over time, $-\pi/2 < \sigma_R(t) < \pi/2$ for $t \in [0, t_f]$. However, this is only a necessary condition. Therefore, it needs to be proved to satisfy the sufficient condition. This proof will be addressed after synthesizing the guidance law.

From Eq. 11, substituting the velocity ratio η, we get the following equation:

$$V_R = V_M \sqrt{1 + \eta^2 - 2\eta \cos(\psi_M - \psi_T)} \tag{20}$$

Based on the expression Eq. 20, it can be seen that V_R changes over time, s positive and the value of V_R is in the following range:

$$\begin{cases} V_R(t) \le (1+\eta)V_M \\ 0 < (1-\eta)V_M \le V_R(t) \end{cases} \tag{21}$$

Accordingly, the initial kinematic model of a missile with constant speed attacking a maneuvering target can be transformed into an alternative model, where the missile has variable speed while the target remains stationary. The main advantage of this transformation is that it allows the construction and solution of guidance laws without the need for linearization. In other words, this method simplifies the guidance system's analysis and design process while enhancing the accuracy and efficiency of guidance algorithms.

Problem formulation

Before getting into the problem formulation, let us first explain two concepts used in synthesizing guidance law: ZEM is understood as the measured distance between the target's center of mass and its projection along the relative velocity direction, assuming that both the target and missile begin moving uniformly from that point in time (Tang *et al.* 2023). In the relative virtual frame in Fig. 3, the ZEM, represented by *ZEM(t)*, can be expressed as:

$$ZEM(t) = r\sin\sigma_R \tag{22}$$

To achieve a perfect intercept of the target, it is necessary to reduce the ZEM to zero at the final time t_f. Therefore, the condition for a successful target intercept is determined as:

$$ZEM(t_f) = 0 \tag{23}$$

In which the symbol t_f represents the interception time.

The preliminary concept of OED

This section provides an overview of finite-time convergence error dynamics. The concept introduced here enables us to achieve convergence of guidance errors within a specified time frame and shape the error pattern as needed. Designing guidance laws tackles a control problem aimed at monitoring and adjusting errors within a finite period. Defining the relevant guidance error, denoted as *e(t)*, is crucial for achieving the intercept condition. This error may take various forms in various forms, such as ZEM, LOS rate, HE, impact time error, or impact angle error, depending on the specific nature of the guidance problem (He and Lee 2018; Jeong *et al.* 2024).

In order to establish the system equations describing the dynamics of the selected guidance error, we derive the guidance error's derivative over time. This derived equation illustrates the progression of the guidance error over time and provides insights into its behavior and attributes. The general form of the system equation is as follows:

$$\dot{e}(t) = g(t)u(t) \tag{24}$$

while *g(t)* is considered a known function that changes over time and *u(t)* is the input control signal of the system.

Recent studies in He and Lee (2018) and Li *et al.* (2018) have explored OED to achieve optimal convergence patterns of guidance errors within a finite time frame. Based on the results in these works, the OED can be expressed as follows.

$$\dot{e}(t) + \frac{\Gamma(t)}{t_{go}}e(t) = 0 \tag{25}$$

where $t_{go} = t_f - t$ denotes the time-to-go, indicating the missile's remaining flight time until the target is intercepted. Equation 25 is a simple form of Cauchy-Euler type differential equation. The analytical solution of the Eq. 25 takes the following form:

$$e(t) = e(t_0)\left(\frac{t_{go}}{t_f}\right)^{\Gamma} \tag{26}$$

From Eq. 26, it can be seen that if $e(t_0)$ is initially non-zero, the error $e(t)$ will approach zero as t_{go} gradually approaches zero. Where $\Gamma > 0$ is the gain that changes over time, characterizing the rate at which the error $e(t)$ converges to zero and is determined as follows:

$$\Gamma(t) = \frac{t_{go} W^{-1}(t) g^2(t)}{\int_t^{t_f} W^{-1}(\tau) g^2(\tau) d\tau} \tag{27}$$

with $W(t) > 0$ is called the weighting function, having arbitrary forms but always being positive.

The control input resulting from the OED described above minimizes the cost function specified below. The full proof, utilizing the Schwarz inequality theorem, has been detailed in (He *et al.* 2020):

$$J = \frac{1}{2}\int_t^{t_f} W(\tau) u^2(\tau) d\tau \tag{28}$$

Guidance law design

Derivation of guidance law with constant guidance gain (RPNG with constant N_p)

The guidance law, formulated with a meaningful cost function, is designed using OED. The control objective aims to devise feedback guidance commands that enable the missile to intercept the target successfully at the designated final time. The guidance error is defined as follows:

$$e_z(t) = 0 - ZEM(t) \tag{29}$$

We define the OED for $e(t)$ as follows:

$$\dot{e}_z(t) + \frac{N_p}{t_{go}} e_z(t) = 0 \tag{30}$$

where N is a positive constant. Substituting Eq. 22 into 29 and then taking the time derivative of the guidance error, we get:

$$\dot{e}_z(t) = -(\dot{r}\sin\sigma_R + r\cos\sigma_R \dot{\sigma}_R) \tag{31}$$

By substituting Eqs. 16–19 into Eq. 31 and performing some simple transformations and rearrangements, we obtain the following result:

$$\dot{e}_z(t) = -\frac{a_R r\cos\sigma_R}{V_R} \tag{32}$$

From Fig. 3, we can roughly estimate the time-to-go as follows: $\hat{t}_{go} \approx \frac{r\cos\sigma_R}{V_R}$; then Eq. 32 takes the following form:

$$\dot{e}_z(t) = -a_R t_{go} \tag{33}$$

In this case, derived from Eq. 24, we obtain the control input *u(t)* and the function *g(t)* as:

$$\begin{cases} g(t) = -t_{go} \\ u(t) = a_R \end{cases} \tag{34}$$

In this case, $\Gamma(t)=N_p$, from Eqs. 27 and 28, we derive the related cost function as:

$$J = \frac{1}{2}\int_t^{t_f} \frac{u^2(\tau)}{t_{go}^{N_p-3}} d\tau \tag{35}$$

By replacing Eq. 30 into Eq. 33, we derive the expression for the guidance law in the case of constant N_p guidance gain as follows:

$$a_R = N_p \frac{ZEM(t)}{t_{go}^2} \approx N_p V_R \dot{\lambda} \tag{36}$$

The guidance law (Eq. 36), formulated within the virtual relative coordinate system, has the similar form as the ideal PNG. However, instead of the variable V_M, it is replaced by the variable V_R in the above expression. From Eq. 35, we see that the performance index represents energy optimization weighted by $1/t_{go}^{N_p-3}$. Choosing $N_p = 3$ ensures OED for energy optimization. Moreover, $N_p > 3$ in the guidance law (Eq. 36) results in zero terminal command acceleration as the weighting function approaches infinity as t_{go} approaches zero. This ensures the missile has sufficient operational margins to handle undesired disturbances as it approaches the target.

Finally, it is important to note that the previous result assumes a decrease in *r(t)* over time. The proposition below offers a sufficient condition to meet this assumption, guaranteeing interception within a finite time.

Proposition

When the guidance law specified in Eq. 36 is applied, the range *r* will monotonically decrease to *0* within a finite time, and thus the relative lead angle will reach *0* within a finite time, if $\eta < 1$ and $-\pi/2 < \sigma_R(0) < \pi/2$.

Proof: substituting Eq. 17 into Eq. 36, we have:

$$a_R = -N_p \frac{V_R^2 \sin\sigma_R}{r} \tag{37}$$

Substituting Eq.37 into Eq.19, we get:

$$\dot{\sigma}_R = -(N_p - 1)\frac{V_R \sin\sigma_R}{r} \tag{38}$$

Divide Eq. 16 by Eq. 38, then rearrange to separate the variables *r* and σ_R on different sides:

$$\frac{\dot{r}}{r} = \frac{1}{(N-1)} \frac{\cos\sigma_R \dot{\sigma}_R}{\sin\sigma_R} \tag{39}$$

Integrating both sides of Eq. 39, we get the following result:

$$\sin\sigma_R(t) = \sin\sigma_{R0}\left(\frac{r(t)}{r_0}\right)^{N-1} \tag{40}$$

From Eq. 40, given the initial conditions $N > 1$ and $\sigma_{R0} \neq 0$, we have $\sin\sigma_R(t) = 0$ if and only if $r(t) = 0$. Given that $r(t)$ is continuous, there must be a finite time t_f where $r(t_f) = 0$. This implies that $r(t)$ decreases monotonically to zero within a finite period. Consequently, $\sigma_R(t)$ also approaches zero within this finite time frame. Q.E.D.

To analyze the physical significance of the guidance command in Eq. 36, we can transform it using Eqs. 22 and 19, using the approximation $sin\sigma_R \approx \sigma_R$. Substituting this expression into Eq. 36 will yield:

$$a_R = \frac{N_p V_R e_h}{t_{go}} \tag{41}$$

where $e_h = \lambda - \Psi_R = -\sigma_R$ can be described as the angular deviation from the heading towards a virtual stationary target (heading angle error) in the virtual reference coordinate system. Hence, this guidance law can be interpreted as a feedback control command for the heading angle error, employing a time-varying proportional gain. Its purpose is to ensure that Ψ_R aligns with λ.

From the expression of the guidance law (Eq. 41), we can see that when the missile attacks the target with a large initial lead angle e_{h0} (the angle between the missile's velocity vector and the LOS to the target), with a constant N coefficient, the initial command acceleration will have to be very large. This phenomenon can lead to exceeding the missile's allowable overload limits. Therefore, measures are needed to reduce sensitivity to the initial lead angle error to ensure safety and effectiveness in cases with a large initial lead angle.

To address this drawback, this paper proposes a suitable weighting function $W(t)$ to optimize the distribution of command acceleration a_R during the guidance phase by adjusting the value of the coefficient N.

Derivation guidance law with a variable guidance gain (RPNG with variable N_p)

In Eq. 28, the theoretical foundation of OED outlines the weighted guidance law, highlighting the importance of a weighting function $W(t) > 0$. This function shapes the optimal control signal by governing its amplitude. When the weighting function's amplitude is large, the control signal's amplitude decreases to minimize the performance index and *vice versa*. Increasing the relative weighting at the beginning and end of the guidance phase reduces initial and final command accelerations compared to uniform weighting. Thus, distributing the weighting function throughout the engagement process allows for precise adjustment of command acceleration.

The OED in this case is given by:

$$\dot{e}_z(t) + \frac{N_p(t)}{t_{go}} e_z(t) = 0 \tag{42}$$

Once the appropriate weighting function $W(t)$ is selected, we derive the guidance gain function $N_p(t)$ from Eq. 27 is as follows:

$$N_p(t) = \frac{t_{go} W^{-1}(t) g^2(t)}{\int_t^{t_f} W^{-1}(\tau) g^2(\tau) d\tau} \tag{43}$$

To ensure that the calculation of the coefficient $N_p(t)$ in the integral of Eq. 43 does not depend on the function $g(t)$, we choose the weighting function in the following form: $W(t) = g^2(t)R(t)$. To implement the aforementioned idea, we propose the weighting function $R(t)$ in the form of a rational polynomial function of t_{go} as follows:

$$R(t) = \frac{1}{at_{go}} + bt_{go} \tag{44}$$

The Eq. 44 indicates that the variables $a > 0$ and $b > 0$ serve as distribution parameters for designing the weighting function. From Eq. 44, the second term dominates initially, resulting in a considerable weighting value. This significant value mitigates sensitivity to the initial HE by reducing the initial guidance command. The second term decreases as t_{go} approaches zero. At the terminal time, the weighting function $R(t)$ also produces a considerable value due to the increase in the first term of Eq. 44. Moreover, the weighting function $R(t)$ exhibits higher or minimum values at specific points in the engagement process than others.

Unlike traditional PNG laws with fixed weights corresponding to constant guidance gain or some guidance laws with weighting functions that monotonically increase as t_{go} decreases, the authors' selected weighting function may display nonmonotonic behavior with extremal points.

This allows designers to adjust relative weighting values over time for the terminal guidance phase by tuning the design parameters a and b. From Eq. 44, it can be shown through straightforward calculations that this proposed weighting function $R(t)$ has a minimum value at $2\sqrt{b/a}$ at $t_{go} = 1/\sqrt{ab}$. Therefore, the boundary of the design parameters to ensure that the minimum value occurs during the engagement process (i.e., $0 \le t \le t_f$) is given by $\sqrt{ab} \ge 1/t_f$.

Simulation results in Fig. 4 for the $R(t)$ function demonstrate that by choosing suitable design parameters a and b, relative weight values can be easily adjusted throughout the entire guidance process. This includes controlling minimum and maximum values, as well as the ratio between initial and terminal values relative to the minimum. In contrast, for a weighting function in the form of $1/t_{go}$, the weight starts at zero during the initial stage and progressively increases in the cost function. The chosen weighting function facilitates the generation of smaller guidance command values at both the start and end of the guidance phase.

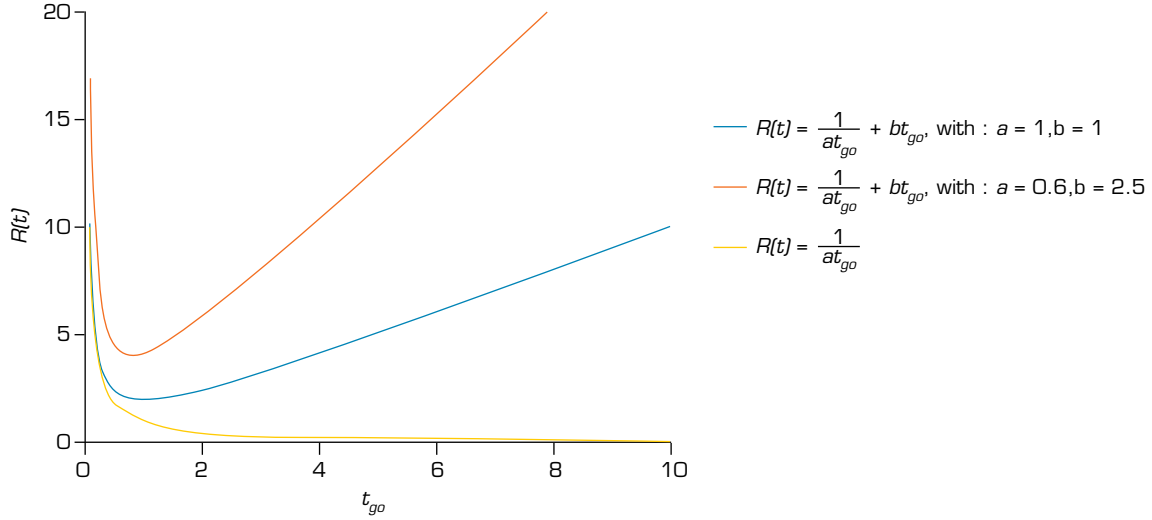

Source: Elaborated by the authors.

Figure 4. Compare the weighting functions and the effects of the design parameters a and b.

Substituting Eq. 44 into Eq. 43, we get the following expression for $N(t)$:

$$N_p(t) = \frac{2ab^2 t_{go}^2}{(1+abt_{go}^2)\ln(1+abt_{go}^2)} \tag{45}$$

The expression of the guidance law (Eq. 36) has been adjusted to account for the time-varying guidance gain N_p, resulting in the following form:

$$a_R = N_p(t)\frac{ZEM(t)}{t_{go}^2} \approx N_p(t)V_R\dot{\lambda} \tag{46}$$

The guidance law in Eq. 46 is derived in a relative virtual coordinate system. To obtain the expression for the command acceleration in the original inertial frame, we substitute Eq. 46 or Eq. 36 into Eq. 15, yielding:

$$a_M = \frac{a_R + a_T\cos(\psi_R - \psi_T) - A_T\sin(\psi_R - \psi_T)}{\cos(\psi_R - \psi_M)} \tag{47}$$

In the case where the target tank is stationary, it follows that $V_R = V_M$ and $\Psi_R = \Psi_M$. Consequently, the synthesized guidance law will precisely become the PNG law:

$$a_M = N_p V_M \dot{\lambda} \tag{48}$$

The guidance law expression (Eq. 47) is of an analytical form, making real-time processing straightforward. To apply this guidance law, besides the predetermined design parameter values such as the guidance coefficient *Np*, variables such as a_T, A_T, and Ψ_T are considered known due to the predetermined motion state of the target. Target information is collected from the tracking system, which typically uses guidance filters (Song *et al.* 1988).

Parameters such as the LOS angular rate, range *r*, missile velocity V_M, time-to-go (t_{go}) parameter, and computed quantities like θ_R, V_R need to be provided. Missile information is obtained from the integrated inertial navigation system (INS), while the LOS rate is measured by the seeker. If the missile uses a gimbaled seeker, the LOS rate can be measured directly; if it uses a strapdown IIR seeker, the LOS rate needs to be estimated using an unscented Kalman filter (Sun *et al.* 2015; Xu *et al.* 2020). The relative distance from the missile to the target can be estimated using infrared imaging information, which is indirectly reflected through the pixels (Yu *et al.* 2017). The t_{go} parameter can also be calculated based on these measured and estimated parameters.

We assume that all necessary information to implement the proposed guidance law has been perfectly obtained. Therefore, if the missile is equipped with a seeker, guidance filter, and INS, the proposed guidance law can be calculated from the measured and estimated information.

Simulations

Survey of the proposed guidance laws

In this section, the author conducts combat scenario simulations to validate the efficacy of the synthesized guidance laws, employing a foreign tank as a hypothetical target. This target tank is highly maneuverable and capable of moving forward-backward and left-right on the ground. The military vehicles in the simulation can turn with an acceleration ranging from 0.3 to 0.5 g and have a braking capability of up to 0.9 g (Gibbs 2011). In the hypothetical scenario, the target tank moves with an initial speed of $V_{T0} = 10$ *m/s,* with a longitudinal acceleration of *1 m/s²*, and performs a wave maneuver to avoid missile attacks, with the acceleration at time t given by $a_T = a_{T0}\sin(\omega t + \psi_{T0} + \pi/2)$. The missile velocity in the simulation is assumed to be

constant, $V_M = 300\ m/s$. These factors are established to create a realistic simulation environment, testing the adaptability and effectiveness of the guidance laws in diverse and complex combat situations. Furthermore, the homing process concludes when the relative range r is less than or equal to 0.5 m in all scenarios.

To solve the system of differential equations from Eqs. 1–10 using numerical simulation in Matlab, we need to incorporate the guidance law expression (Eq. 47) into the solution process. Before proceeding, the initial values of the parameter variables must be provided. Some initial conditions are given in Table 1, and the initial values for variables such as r_0, λ_0 and the initial heading angle of the missile Ψ_{M0} need to be calculated from other initial parameters. This ensures that we have complete and accurate initial conditions for the simulation process.

Table 1. Simulation setting.

Parameters	Values
Initial position of the missile ($x_M(0)$, $z_M(0)$)	(0, 0) m
Initial position of the target ($x_T(0)$, $z_T(0)$)	(2,000, 100) m
Missile speed V_M	300 m/s
HE	-30 ~ 30 deg
Missile acceleration limits $\|a_M\|$max	10 g
Initial velocity of the target V_{TO}	10 m/s
Axial acceleration of target A_T	1 m/s²
The initial heading angle of the target Ψ_{TO}	2 π/6 rad
Maneuver magnitude of target a_{TO}	5 m/s²
Natural frequency of target ω	1,256 rad/s

Source: Elaborated by the authors.

where:

$$r_0 = \sqrt{\left(x_{T0} - x_{M0}\right)^2 + \left(z_{T0} - z_{M0}\right)^2} \tag{49}$$

$$\lambda_0 = \tan^{-1}\frac{\left(z_{T0} - z_{M0}\right)}{\left(x_{T0} - x_{M0}\right)} \tag{50}$$

We need to calculate the initial lead angle to determine the initial trajectory heading angle of the missile Ψ_{M0}. This angle, known as the missile lead angle L_0, is the angle between the missile's velocity vector and the initial LOS. The theoretical missile lead angle can be calculated by applying the law of sines, yielding the following result:

$$L_0 = \sin^{-1}\frac{V_{T0}\sin(\psi_{T0} + \lambda_0)}{V_M} \tag{51}$$

At that point, the initial trajectory-heading angle of the missile is calculated as follows:

$$\psi_{M0} = \lambda_0 + L_0 + HE \tag{52}$$

In this context, the HE indicates the initial angular deviation of the missile relative to the collision triangle (Tanriverdi and Cavdaroglu 2017).

We will conduct numerical simulations to evaluate the effectiveness of the proposed guidance laws in two scenarios: with a constant N_p factor and an N_p factor that varies according to the weight function $R(t)$. Both scenarios use the same input parameter values in Table 1 and are examined with an initial HE ranging from -30 to 30 degrees. For the case of a constant N_p factor, the chosen value is $N_p = 3$. For the scenario where the N_p factor varies, the authors selected parameters $a = 0.5$ and $b = 2.5$ for the weight function $R(t)$.

The simulation results shown in Fig. 5 indicate that both the RPNG law with constant N_p and the RPNG law with variable N_p successfully intercept the target with zero final miss distance. The graphs of the look angle over time converge to zero, demonstrating that the target approach conditions analyzed earlier are met.

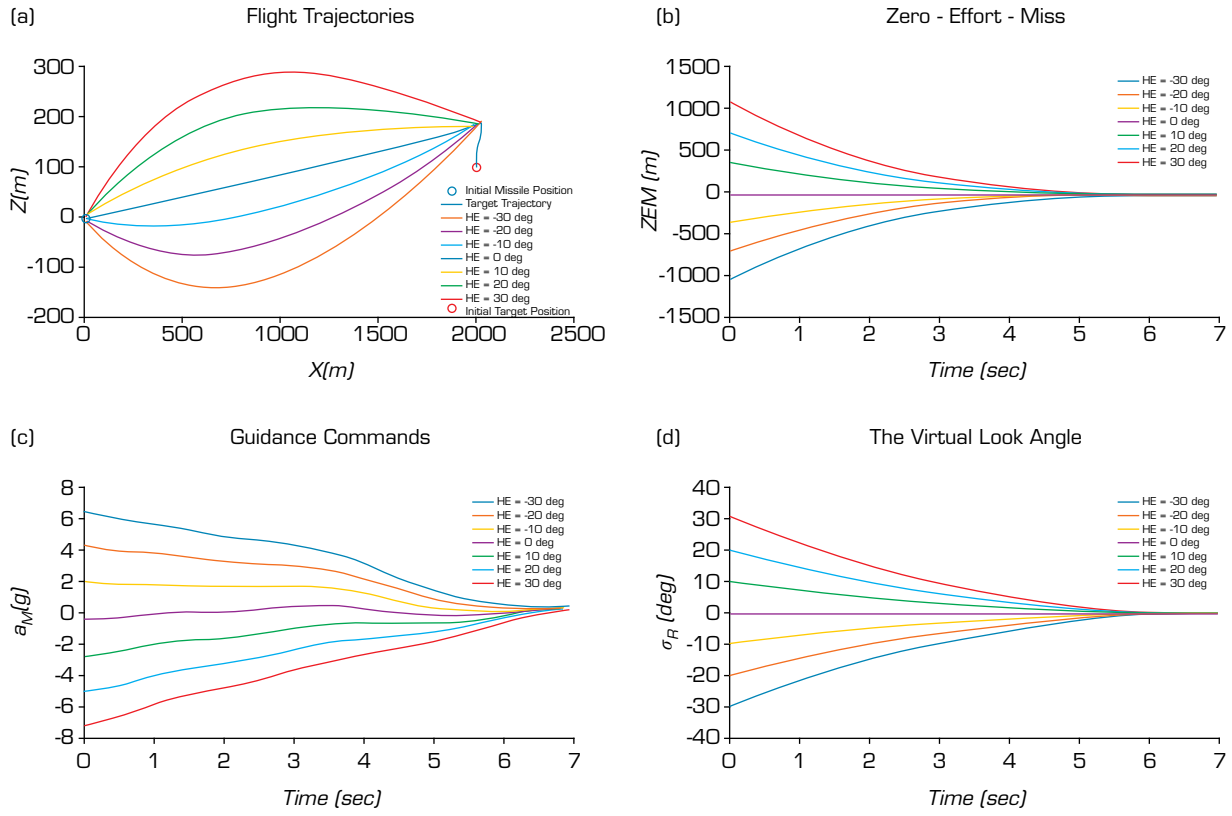

Source: Elaborated by the authors.

Figure 5. Simulation Results of the RPNG law with constant N_p.

The difference between the RPNG law with variable N_p and the RPNG law with constant N_p is highlighted in the missile's command acceleration graph. Specifically, the RPNG law with variable N_p, where the guidance coefficient N_p is distributed according to the weighting function $R(t)$, shows a lower initial command acceleration than the RPNG law with constant N_p. This difference is particularly noticeable when the initial HE angle is large.

The graph of the guidance coefficient N_p for the RPNG law with variable N_p in Fig. 6d shows that N_p changes over time, starting from a low value and reaching five at the final time, in contrast to the constant $N_p = 3$ for the RPNG law with constant N_p. Therefore, the RPNG law with variable N_p is more effective in scenarios with large initial HE angles, as it reduces the initial command acceleration during the homing phase, avoiding abrupt command changes during the transition between guidance phases and preventing overload on the missile's control actuators.

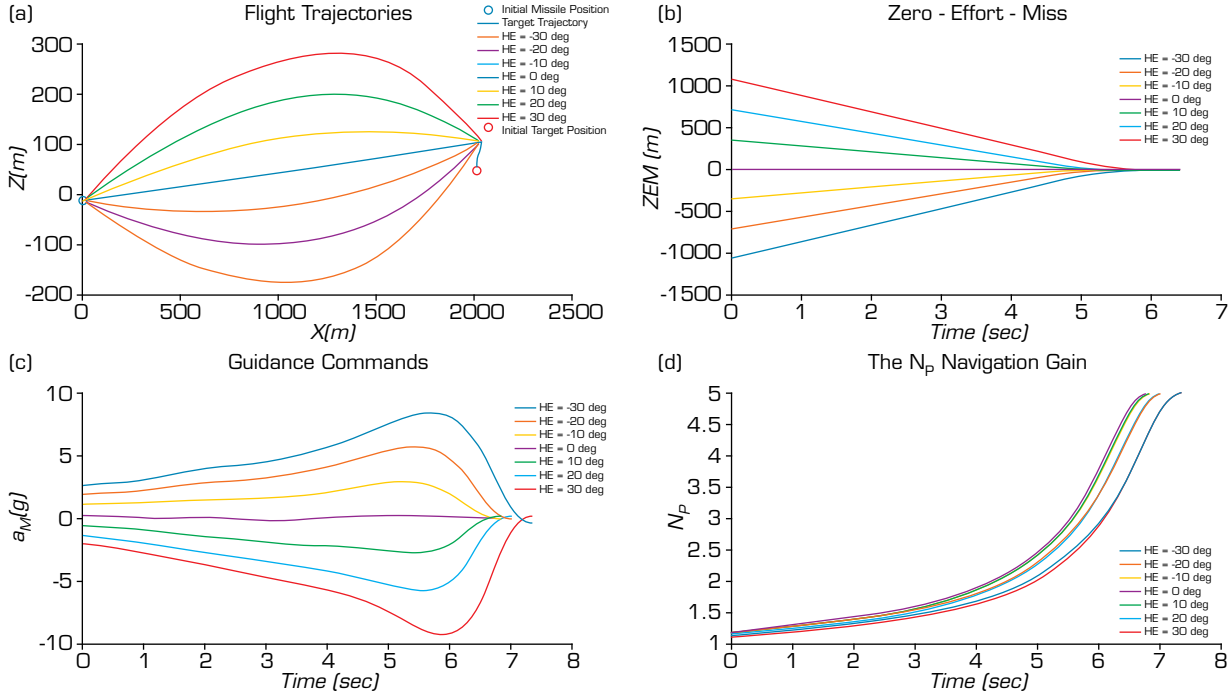

Source: Elaborated by the authors.

Figure 6. Simulation results of the RPNG law with variable N_p.

Monte Carlo simulation

In practice, uncertainties due to measurement errors and environmental noise always exist, combined with the missile system's autopilot lag and acceleration limits, causing significant miss distance and resulting in missile performance degradation. To address this issue, the guidance law needs to be highly robust. A Monte Carlo simulation with 500 runs has been conducted to demonstrate the robustness of the proposed guidance laws and compare the average ZEM and control energy of these proposed guidance laws with the APNG law. The simulation conditions include the initial positions of the target and missile as per Table 1, HE set to 20 degrees; other initial parameters were randomly chosen according to a uniform distribution on $[0,1]$, with lower and upper limits as listed in Table 2. The autopilot system is modeled as a first-order lag system as follows:

$$\frac{a_M}{a_c} = \frac{1}{s\tau + 1} \tag{53}$$

Table 2. Lower and upper limits of some initial parameters.

Parameter	Lower limit	Upper limit	Parameter	Lower limit	Upper limit
V_M	250 m/s	300 m·s	A_T	0 m/s²	2 m/s²
V_{TO}	8 m/s	12 m·s	a_M	3 m/s²	5 m/s²

Source: Elaborated by the authors.

In this model, a_M represents the achieved missile acceleration, a_c is the commanded missile acceleration, and τ denotes the time constant of the flight-control system. Due to practical limitations in actuator dynamics in real engineering applications, the maximum lateral acceleration is constrained as follows:

$$a_M = \begin{cases} a_{M\max} sign(a_M) \ if \ |a_M| \geq a_{M\max} \\ a_M \ if \ |a_M| < a_{M\max} \end{cases} \tag{54}$$

We select the first-order time constant as $\tau = 0.3$ seconds and limit the missile's acceleration command to a maximum of ± 10 g.

The APNG law, when transformed to be perpendicular to the missile's velocity vector, will have the following form:

$$a_{APNG} = \frac{N_p V_C \dot{\lambda} + N/2\, a_T \cos(\psi_T - \lambda)}{\cos(\psi_M - \lambda)} \tag{55}$$

The Monte Carlo simulation results of the guidance methods RPNG with variable *Np*, RPNG with constant *Np*, and APNG are presented through scatter plots of the final miss distance values (ZEM) and cumulative distribution plots of the ZEM values, corresponding to Figs. 7–9, respectively.

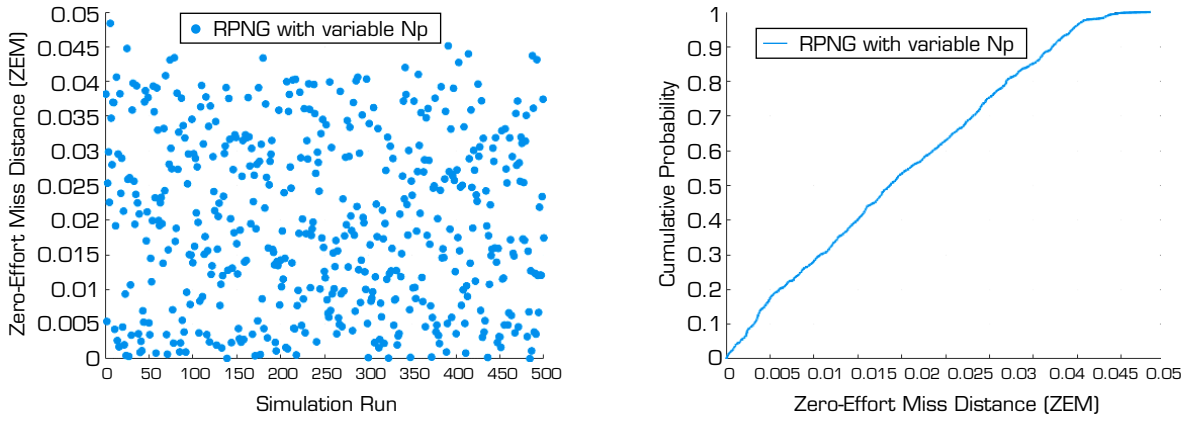

Source:

Figure 7. Monte Carlo simulation result of *RPNG* with variable N_p. (a) scatter diagram of ZEMs; (b) cumulative distribution of ZEMs.

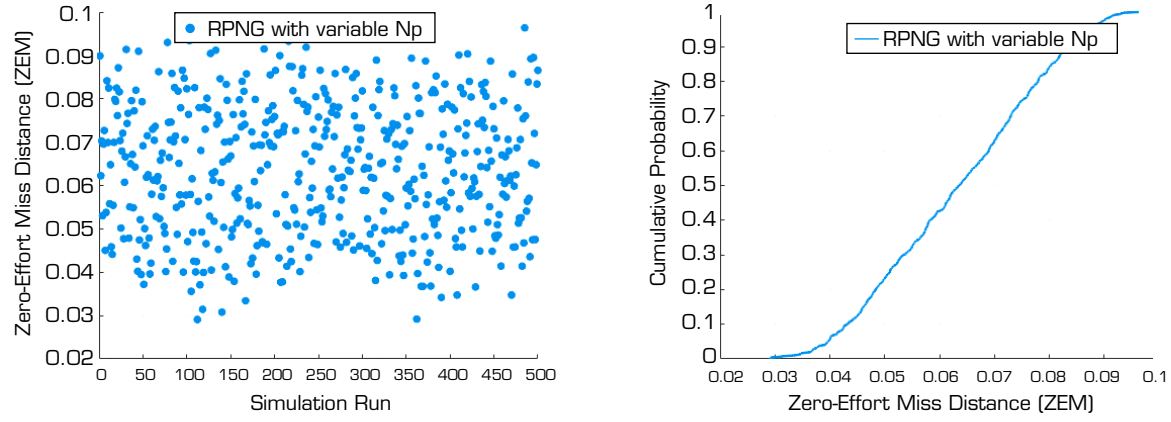

Source: Elaborated by the authors.

Figure 8. Monte Carlo simulation result of RPNG with constant N_p. (a) scatter diagram of ZEMs; (b) cumulative distribution of ZEMs.

The scatter plots illustrate the distribution of final miss distance values between the missile and the target in different simulations, helping us to understand the variability and dispersion of the miss distances under the influence of varying input parameters.

Meanwhile, the cumulative distribution plots of *ZEM* show the percentage of simulations that achieved a *ZEM* value below a certain threshold. This provides a comprehensive view of the effectiveness and reliability of the guidance system, thereby evaluating its ability to achieve the desired accuracy in practice.

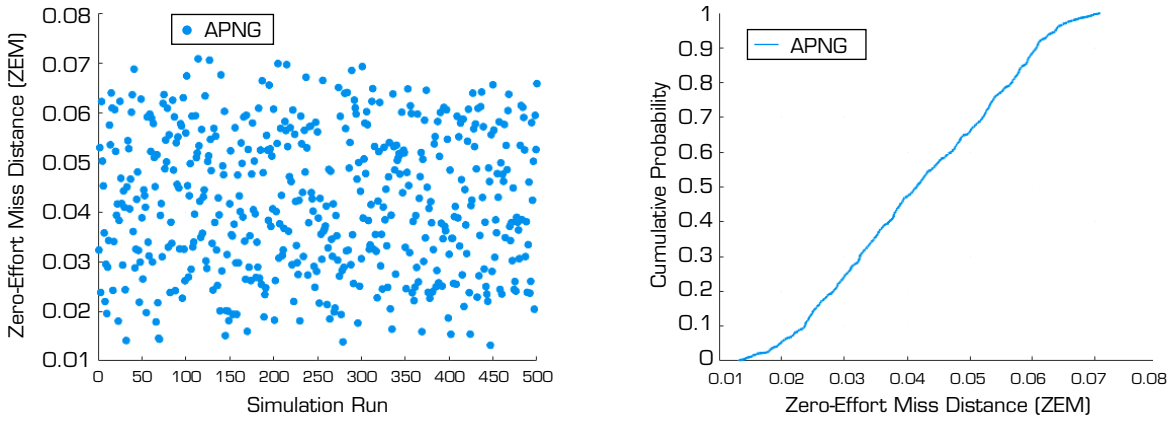

Source: Elaborated by the authors.

Figure 9. Monte Carlo simulation result of APNG. (a) scatter diagram of ZEMs; (b) cumulative distribution of ZEMs.

Table 3 presents the statistical results of the average terminal miss distance and average control effort for the guidance laws *RPNG* with variable *Np*, *RPNG* with constant *Np*, and *APNG* after 500 Monte Carlo simulation runs. Specifically, Table 3 shows:

Average ZEM (m): the average value of *ZEM* measures the average terminal miss distance by which the missile misses the target after applying different guidance laws. These values reflect the accuracy of the guidance laws in controlling the missile to approach the target.

Average control effort (m^2/s^3): the average value of control effort indicates the energy the system uses to control the missile. This value provides information about the performance and energy efficiency of the guidance laws. The control energy consumption for each simulation run is defined as: $\int_0^{t_f} \|a_M\|^2 \, d\tau$

Table 3. Results of Monte Carlo simulation.

Guidance laws	APNG	RPNG (N constant)	RPNG (variable N)
Average ZEM (m)	0.0478	0.0621	0.0215
Average control effort (m^2/s^3)	2752.93	3252.93	1082.52

Source: Elaborated by the authors.

Based on the Monte Carlo simulation outcomes depicted in Figs. 7–9 and the average miss distance results in Table 3, it is evident that the final miss distance for all three guidance laws is relatively small, with a narrow dispersion of miss distance values. This meets the missile guidance requirements given the initial conditions and the variations in input parameters. However, when comparing the methods, we find that the *RPNG* guidance law with variable *Np* is the most effective, with the smallest average miss distance and the lowest control energy required. The *ZEM* scatter plot and the cumulative distribution plot of *ZEM* values show that the final miss distance does not exceed 0.05 m with 100% probability.

Following this, the *APNG* guidance law has a final miss distance not exceeding 0.08 m with 100% probability. Lastly, the *RPNG* guidance law with constant *Np* has a final miss distance not exceeding 0.1 m with 100% probability and requires the highest control energy.

The simulation results show that the weighting function *W(t)* effectively adjusts the guidance coefficient N_p, providing a reasonable distribution of command acceleration and reducing the initial acceleration. This is particularly useful when the missile's heading is far from the collision course. As a result, the control energy required for the *RPNG* guidance law with variable N_p is minimized. On the other hand, when there is a significant initial heading angle error, the term $\cos(\psi_M - \lambda)$ in Eq. 55 of the APNG guidance law becomes small, leading to a higher required command acceleration and, consequently, higher demand for control energy.

CONCLUSION

This paper introduces a new nonlinear optimal guidance law for ATGM to effectively intercept maneuvering tank targets. Using a nonlinear relative model in a two-dimensional horizontal plane and optimizing error dynamics significantly improves traditional methods, transforming moving targets into stationary ones, thereby simplifying the guidance law design process.

Including a time-decay weighting function optimizes the distribution of command accelerations, reducing initial requirements and converging to zero or near zero at the end time. Numerical simulations and Monte Carlo analyses confirm this guidance law's superior performance and robustness, with smaller average miss distances and lower control energy compared to existing methods. However, the study has limitations, such as assuming known target maneuvering information. Future research will expand to three-dimensional scenarios and integrate real-time target information estimation to enhance practical applicability. This study significantly contributes to missile guidance technology, providing a robust solution for ATGM to intercept maneuvering targets with high accuracy and efficiency.

AUTHORS' CONTRIBUTION

Conceptualization: Van HT; **Methodology:** Ngoc DN; **Validation:** Trung DP; **Writing - Original draft:** Van HT; **Writing - Review & editing:** Van HT and Nguyen TT; **Final approval:** Van HT.

CONFLICT OF INTEREST

Nothing to declare.

DATA AVAILABILITY STATEMENT

All data sets were generated or analyzed in the current study.

FUNDING

Not applicable.

ACKNOWLEDGEMENTS

Not applicable.

REFERENCES

Becker K (1990) Closed-form solution of pure proportional navigation. IEEE Trans Aerosp Electron Syst 26(3):526-533. https://doi.org/10.1109/7.106131

Bin YH, Wang DL, Wang Y, Sun X (2023) Impact time control guidance against maneuvering targets based on a nonlinear virtual relative model. Chin J Aeron 36(7):444-459. https://doi.org/10.1016/j.cja.2023.03.014

Dwivedi P, Bhale P, Bhattacharyya A, Padhi R (2016) Generalized estimation and predictive guidance for evasive targets. IEEE Trans Aerosp Electron Syst 52(5):21111-22122. https://doi.org/10.1109/TAES.2016.140861

Gibbs BP (2011) Modeling examples. Advanced Kalman filtering, least-squares and modeling. New Jersey: John Wiley & Sons.

He S, Lee C-H (2017) Gravity-turn-assisted optimal guidance law. J Guid Control Dyns 41(1):171-183. https://doi.org/10.2514/1.G002949

He S, Lee C-H (2018) Optimality of error dynamics in missile guidance problems. J Guid Control Dyns 41(7):1624-1633. https://doi.org/10.2514/1.G003343

He S, Lee CH, Shin HS, Tsourdos A (2020) Optimal guidance and its applications in missiles and UAVs. New York: Springer International Publishing.

He S Song T, Lin D (2017) Impact angle constrained integrated guidance and control for maneuvering target interception. J Guid Control Dyns 40(10):2653-2661. https://doi.org/10.2514/1.G002201

Jeon I-S, Cho H, Lee J-I (2015) Exact guidance solution for maneuvering target on relative virtual frame formulation. J Guid Control Dyns 38(7):1330-1340. https://doi.org/10.2514/1.G000932

Jeong ET, Wang P, He S, Kim TH, Lee CH (2024) Heading error shaping guidance laws using generalized finite-time convergence error dynamics. IEEE Trans Aerosp Electron Syst:60(3):1-16. https://doi.org/10.1109/TAES.2024.3361432

Lee C-H, Kim T-H, Tahk M-J (2013) Interception angle control guidance using proportional navigation with error feedback. J Guid Control Dyns 36(5):1556-1561. https://doi.org/10.2514/1.58454

Lee J-Y, Kim HJ (2021) Impact angle guidance law to prevent the detection degradation of a seeker. Proceedings of the Institution of Mechanical Engineers, Part G. J Aerosp Eng 236(9):1738-1750. https://doi.org/10.1177/09544100211044036

Li B, Lin D, Wang J, Tian S (2018) Guidance law to control impact angle and time based on optimality of error dynamics. Proceedings of the Institution of Mechanical Engineers, Part G: J Aerosp Eng 233(10):3577-3588. https://doi.org/10.1177/0954410018801226

Ratnoo A, Ghose D (2010) Impact angle constrained guidance against nonstationary nonmaneuvering targets. J Guid Control Dyns 33(1):269-275. https://doi.org/10.2514/1.45026

Song TL, Ahn JY, Park C (1988) Suboptimal filter design with pseudomeasurements for target tracking. IEEE Trans Aerosp Electron Syst 24(1):28-39. https://doi.org/10.1109/7.1033

Sun T, Chu H, Zhang B, Jia H, Guo L, Zhang Y, Zhang M (2015) Line-of-sight rate estimation based on UKF for strapdown seeker. Math Probl Eng 2015(1):185149. https://doi.org/10.1155/2015/185149

Tang X, Yu J, Peng S, Dong X, Li Q, Ren Z (2023) Impact angle control guidance for a moving target with general field-of-view constraints. Paper presented 2023 42nd Chinese Control Conference (CCC). IEEE; Tianjin, China. https://doi.org/10.23919/CCC58697.2023.10239807

Tanriverdi G, Cavdaroglu M (2017) Utilization of INS measurements into fixed-point smoothing approach to mitigate the disturbance effect of missile initial heading errors on missile terminal guidance performance. Paper presented 2017 AIAA Guidance, Navigation, and Control Conference. AIAA; Grapevine, USA. https://doi.org/10.2514/6.2017-1033

Tran Van H, Ngoc ND, Van VB, Trung DP, Thanh TN (2023) Synthesis of suboptimal guidance law for anti-tank guided missile with terminal impact angle constraint based on the SDRE technique. Archives of Advanced Engineering Science 2(1):64-70. https://doi.org/10.47852/bonviewAAES32021096

Van HT, Ngoc DN, Dung PT (2023) Field-of-view and impact angle constrained guidance law for missile with reducing sensitivity on initial errors based on optimal error dynamics. Paper presented 2023 12th International Conference on Control, Automation and Information Sciences. IEEE: Hanoi, Vietnam. https://doi.org/10.1109/ICCAIS59597.2023.10382396

Xu Z, Luo H, Hui B, Chang Z (2020) A novel LOS rate estimation method based on images for strap-down inertial guidance. J Phys Conf Ser 1570(1):012060. https://doi.org/10.1088/1742-6596/1570/1/012060

Yu Y, Yi K, Li Q, Dong X, Ren Z (2017) Guidance information estimation of the semi-strapdown infrared imaging seeker. Paper presented 2017 36th Chinese Control Conference. IEEE; Dalian, China. https://doi.org/10.23919/ChiCC.2017.8028341.

Zarchan P (2012) Tactical and strategic missile guidance. Reston: American Institute of Aeronautics and Astronautics. https://doi.org/10.2514/4.868948

Zhou D, Sun S, Teo KL (2009) Guidance laws with finite time convergence. J Guid Control Dyns 32(6):1838-1846. https://doi.org/10.2514/1.42976